

Supplemental Data

Mosaic Uniparental Disomies and Aneuploidies

as Large Structural Variants of the Human Genome

Benjamín Rodríguez-Santiago, Nuria Malats, Nathaniel Rothman, Lluís Armengol, Montse Garcia-Closas, Manolis Kogevinas, Olaya Villa, Amy Hutchinson, Julie Earl, Gaelle Marenne, Kevin Jacobs, Daniel Rico, Adonina Tardón, Alfredo Carrato, Gilles Thomas, Alfonso Valencia, Debra Silverman, Francisco X. Real, Stephen J. Chanock, and Luis A. Pérez-Jurado

Figure S1. Flow chart for CNV analysis with quality control and statistical filtering

Figure S2. Flow chart for genome-wide analysis to detect mosaic rearrangements (UPDs, CNVs and trisomies)

Figure S3. SNP array plots and experimental validation of mosaic rearrangements

Table S1. Mean and standard deviation (SD) of log R ratio (LogR), B-deviation (Bdev) and B-deviation of heterozygous SNPs (HetBdev) per autosomal chromosome of the 1,991 samples analysed.

Table S2. Mosaic rearrangements detected in cases and controls, divided by categories, including information on the validation methods used (microsatellites, MLPA and/or FISH), the chromosomal coordinates and size of the rearrangement, and the actual LogR and HetB-dev values obtained with the SNP array

Table S2A. Mosaic uniparental disomies detected showing normal LogR (copy number neutral) and abnormal heterozygous B-deviation parameters when compared to the genome-wide hybridization data of the sample and to the whole dataset

Table S2B. Mosaic copy number change rearrangements affecting autosomes

Table S3. Statistical tests for case-control comparisons of mosaic rearrangement frequency and proportion of cells carrying the rearrangement

Table S4. Genomic location and sequence characteristics of the breakpoint (BP) intervals for each somatic rearrangement

Table S5. Coordinates of MLPA and FISH probes and microsatellite PCR products (hg18 assembly)

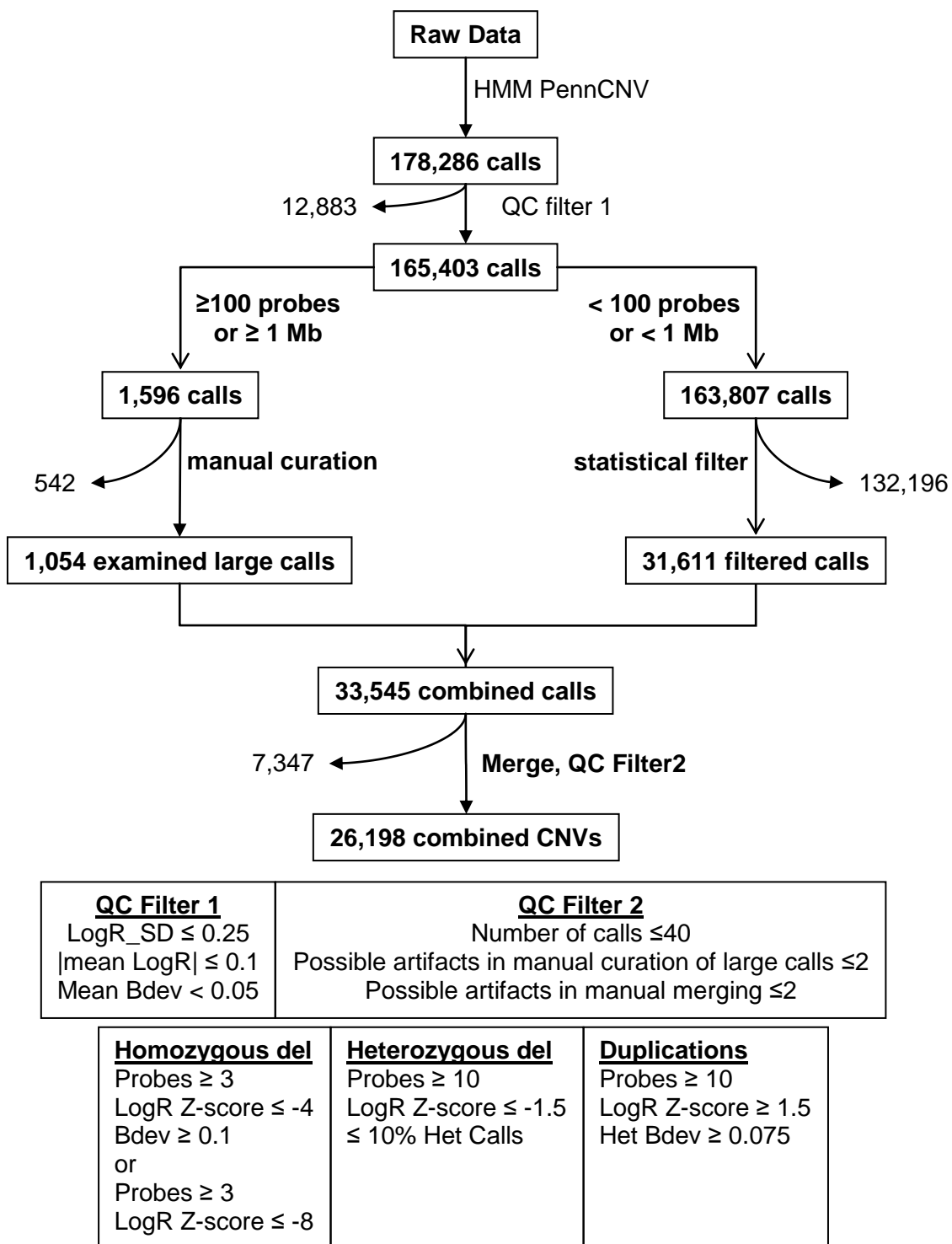


Figure S1. Flow Chart for CNV Analysis with Quality Control and Statistical Filtering

The number of calls discarded and remaining after each step is indicated. A detailed description of the CNV calling procedure has been described elsewhere (Itsara et al., *American Journal of Human Genetics* 84, 148-161, 2009) and may also be found in the methods section.

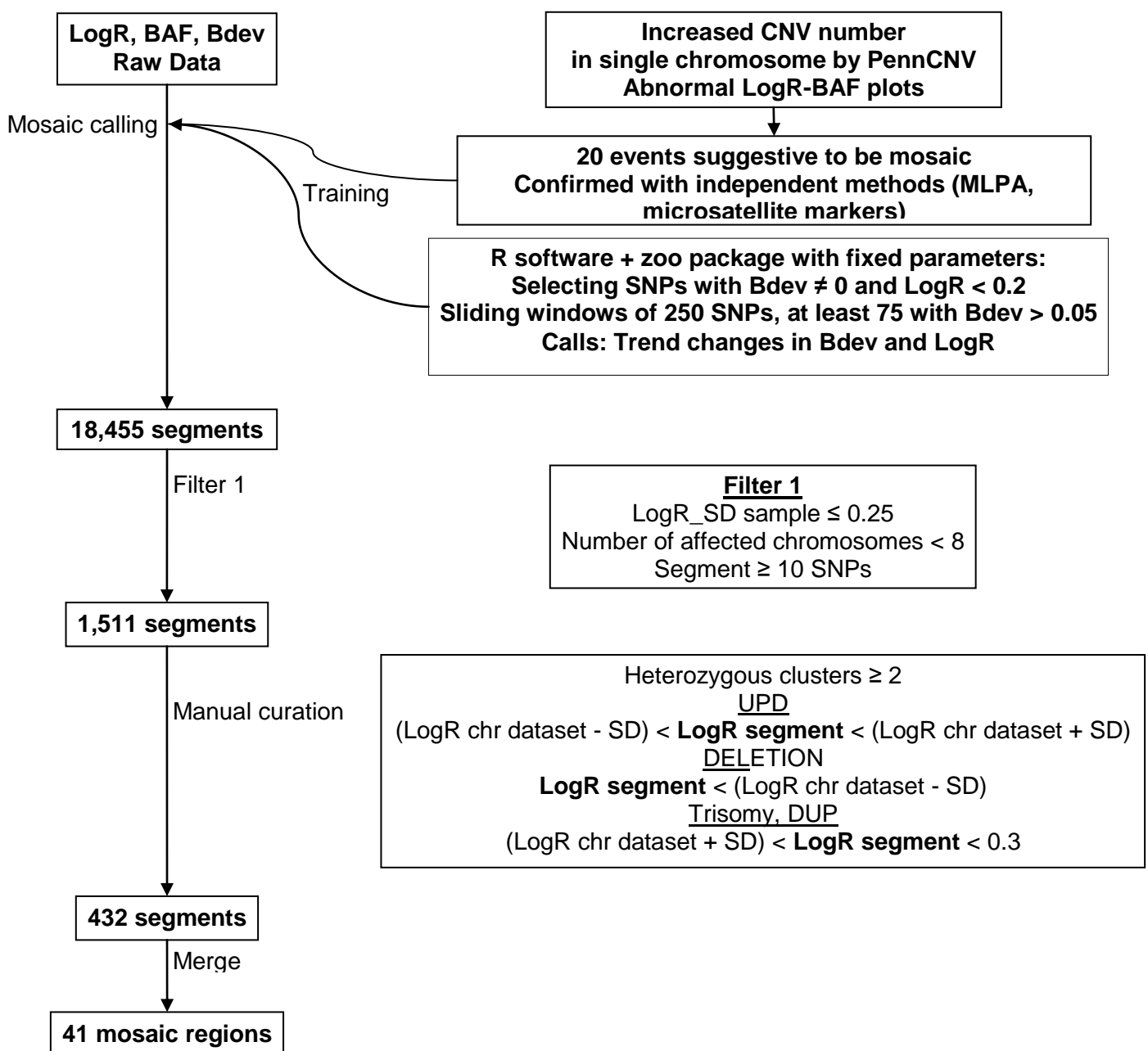


Figure S2. Flow Chart for Genome-wide Analysis to Detect Mosaic Rearrangements (UPDs, CNVs, and Trisomies)

After detecting 20 regions with an elevated number of CNVs in a single chromosome suspected of mosaic events, a specific bioinformatic tool was designed. A detailed description of the procedure may be found within the manuscript. This tool was first set up and trained with those 20 samples, obtaining a 95% detection rate without false positives in the remaining chromosomal regions. The method was then applied to the whole dataset, using filter 1 to discard low quality hybridizations. All segments were manually curated following the presented criteria. Finally, segments within 1 Mb were manually merged.

Figure S3. SNP Array Plots and Experimental Validation of Mosaic Rearrangements

The plot images show the LogR ratio (black dots, scale on the left side) and BAF (red dots, scale on the right side) values of each of the chromosomes identified carrying mosaic rearrangements. Samples' identifiers and chromosome numbers are shown on top of the plot. The corresponding independent experimental validation (when performed), comparing the sample to the wild-type (wt) pattern, is displayed at the side of each plot. The interpretations are summarized at the bottom of each page. Supplementary Table S6 shows the genome coordinates (hg18) for the microsatellite markers and MLPA probes used for validation of the different rearrangements.

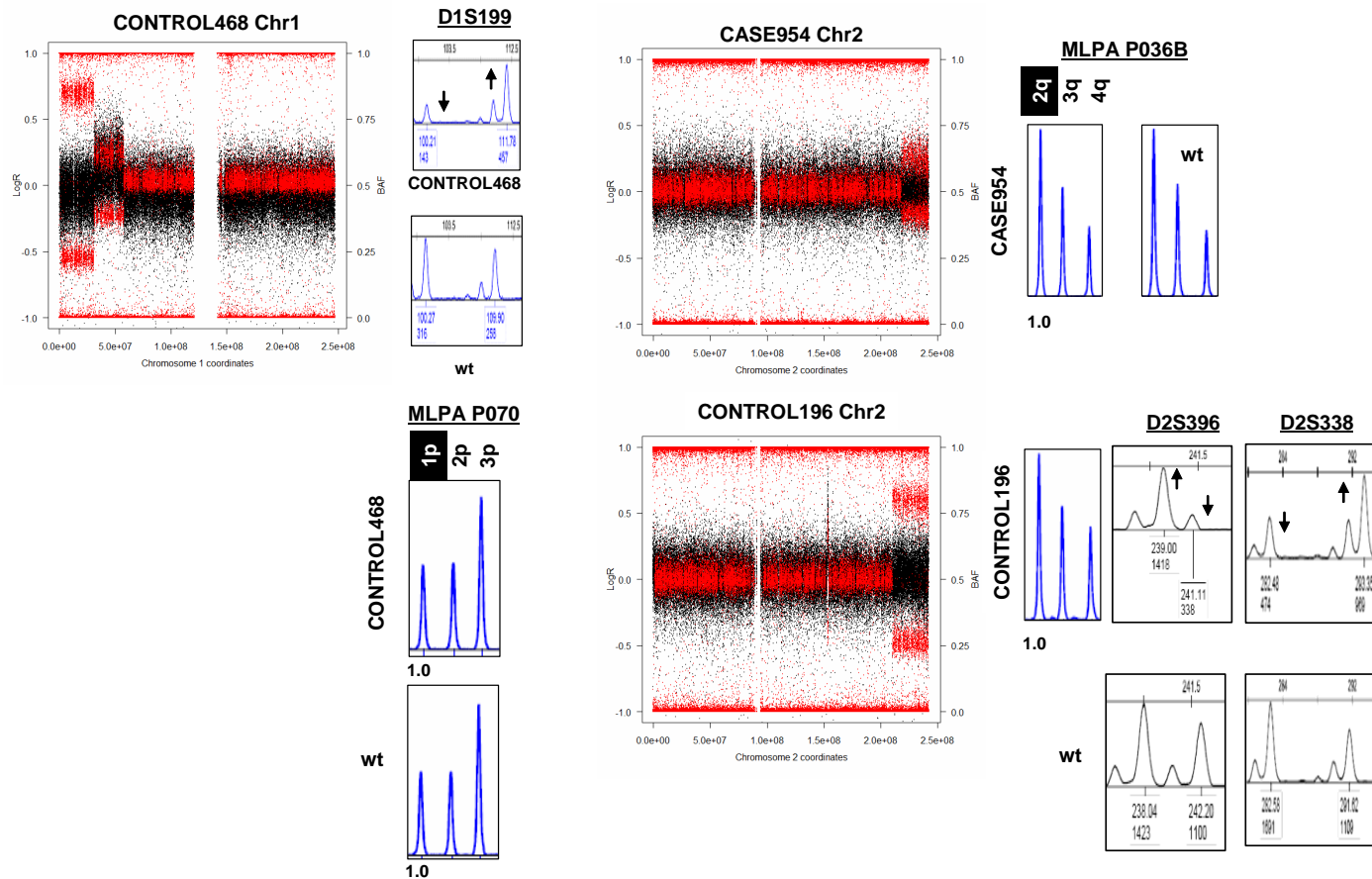


Figure S3A. Mosaic UPDs

CONTROL468: segmental 1p UPD; CASE954 and CONTROL196 segmental 2q UPD. MLPA confirmed the disomic state at the UPD loci with no gain or loss of genetic material (~1.0 RPH). Microsatellite analysis ratified the allelic imbalance in blood DNA reflected by an aberrant ratio between allelic peaks (arrows) with respect to the wild type pattern.

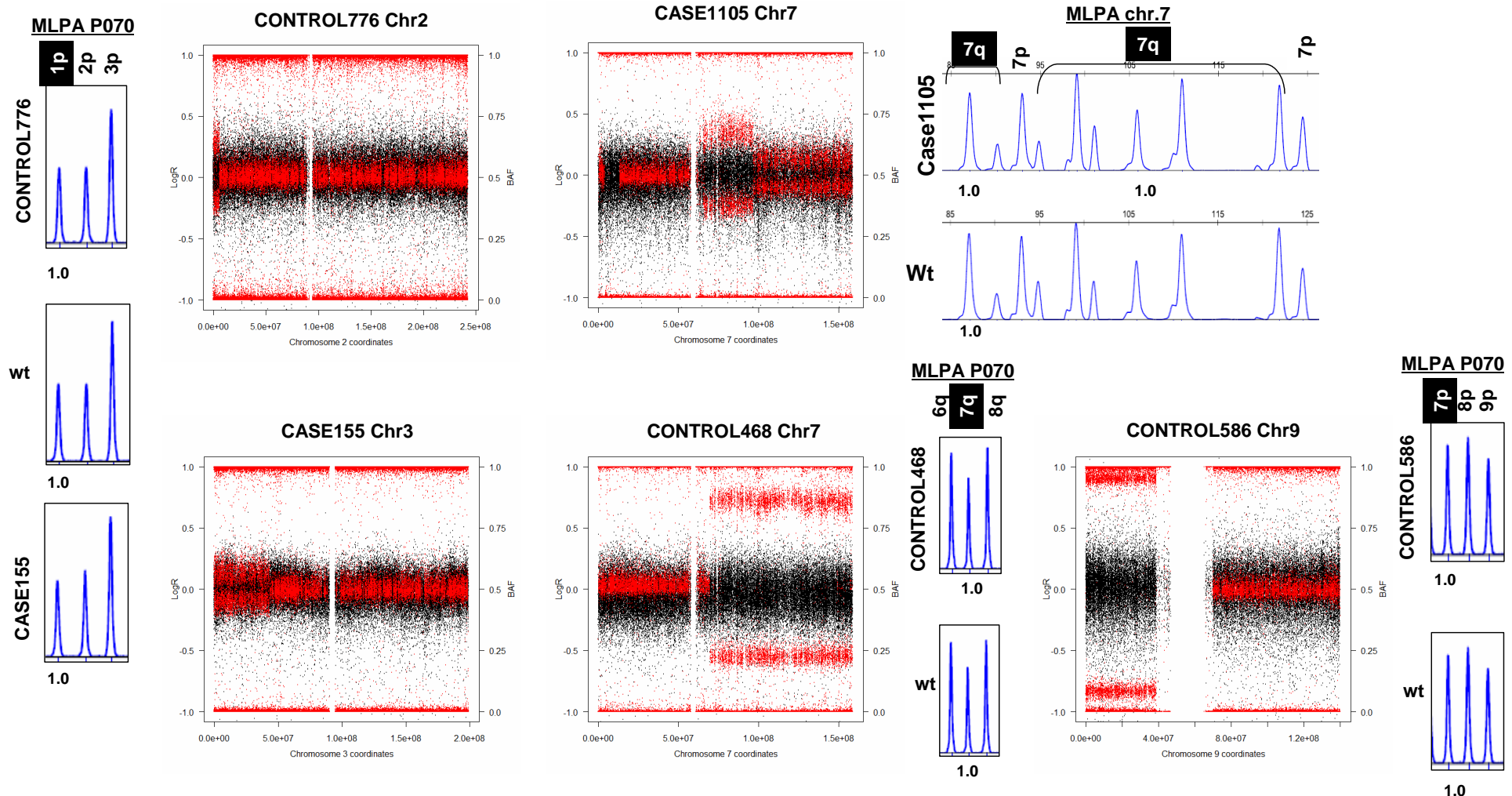


Figure S3B. Mosaic UPDs

Mosaic segmental UPDs at chromosomes 2p in CONTROL776, 7q in CASE1105 and CONTROL468, 3p in CASE155, and 9p in CONTROL586. MLPA with specific regional probes revealed values consistent with a disomic state at the UPD loci, showing no gain or loss of genetic material (~1.0 RPH) in all cases.

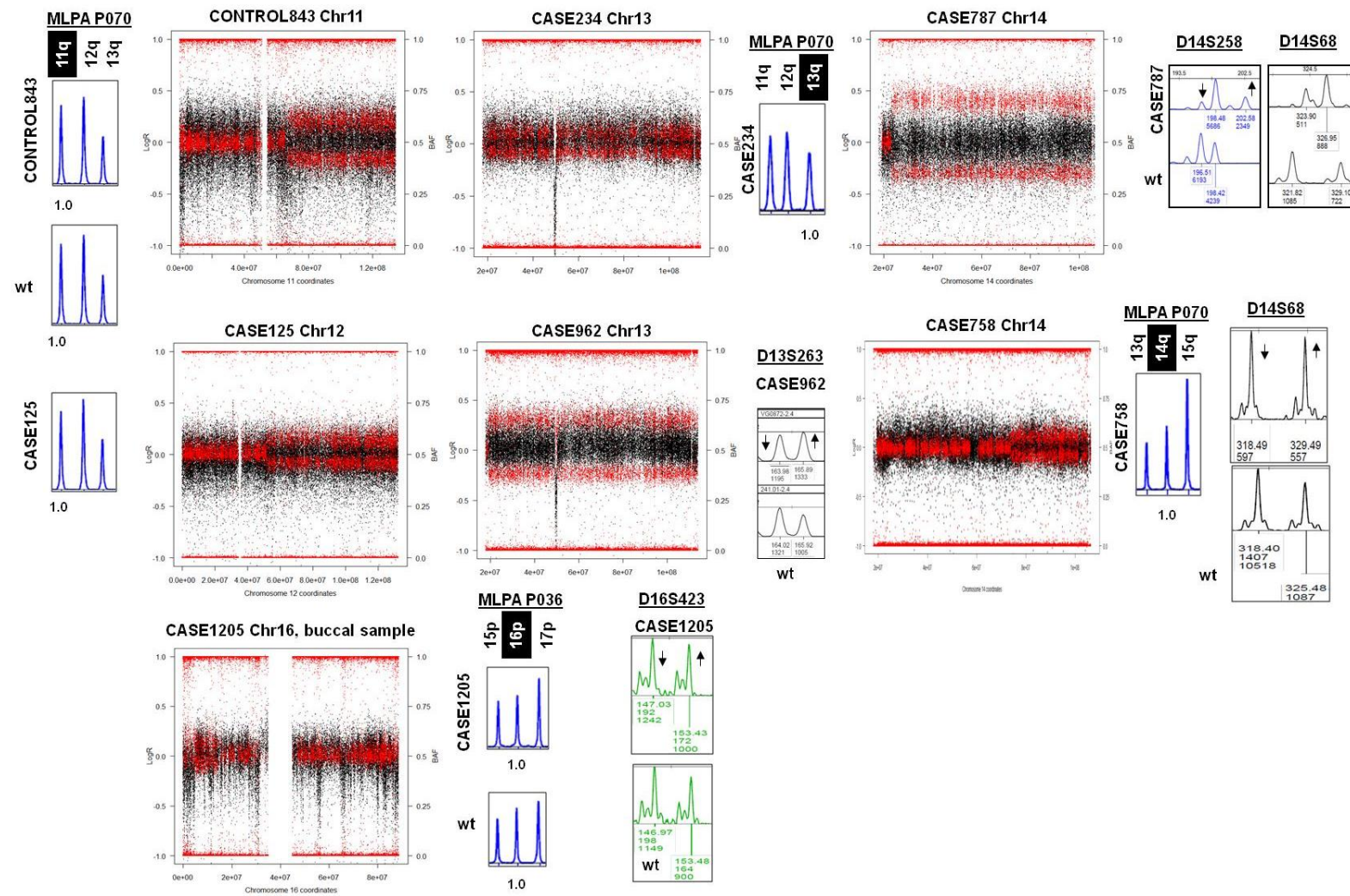


Figure S3C. Mosaic UPDs

Mosaic UPDs at 11q in CONTROL843, 12q in CASE125, 13q in CASE234 and CASE962, 14q in CASE787 and CASE758, and 16p in CASE1205. MLPA confirmed the disomic state at the UPD loci with no gain or loss of genetic material (~1.0 RPH) and microsatellite analysis in CASE962 ratified the allelic imbalance in blood DNA reflected by an aberrant ratio between allelic peaks with respect to the wild type pattern.

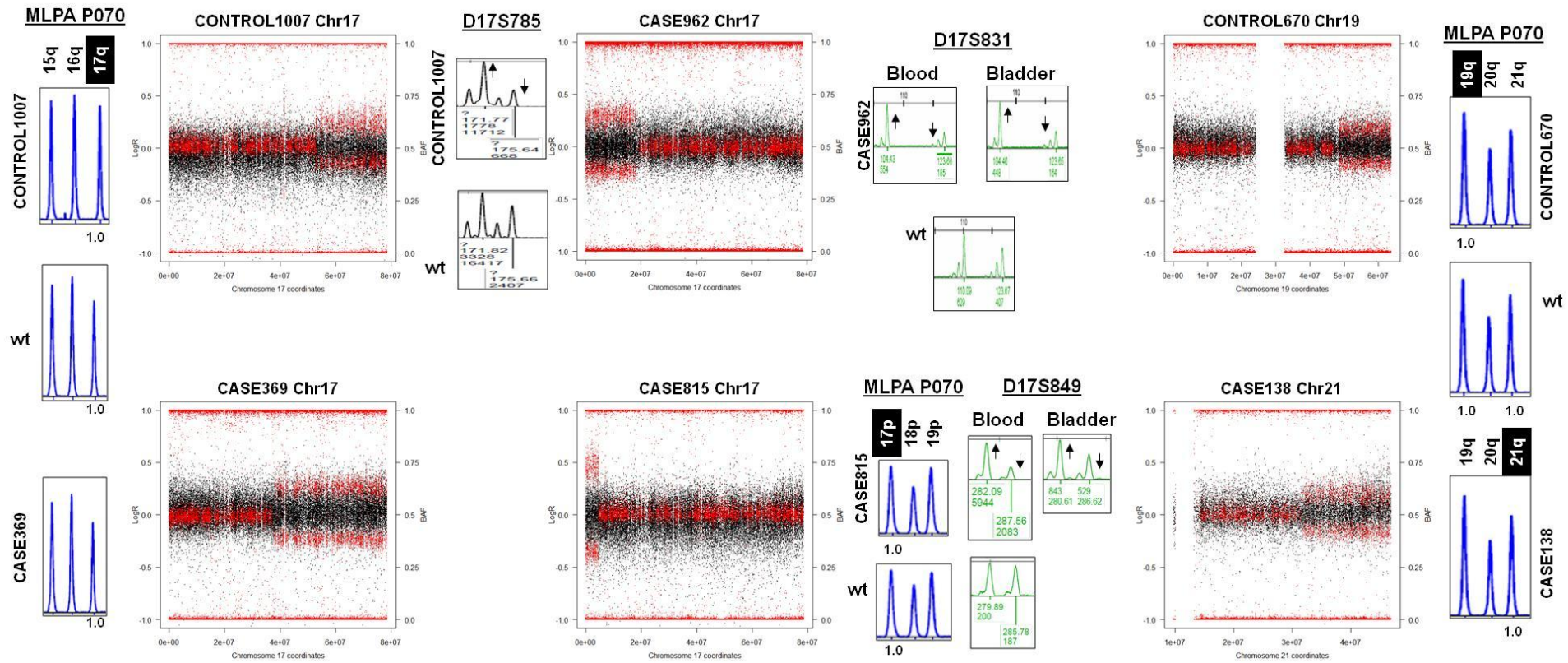
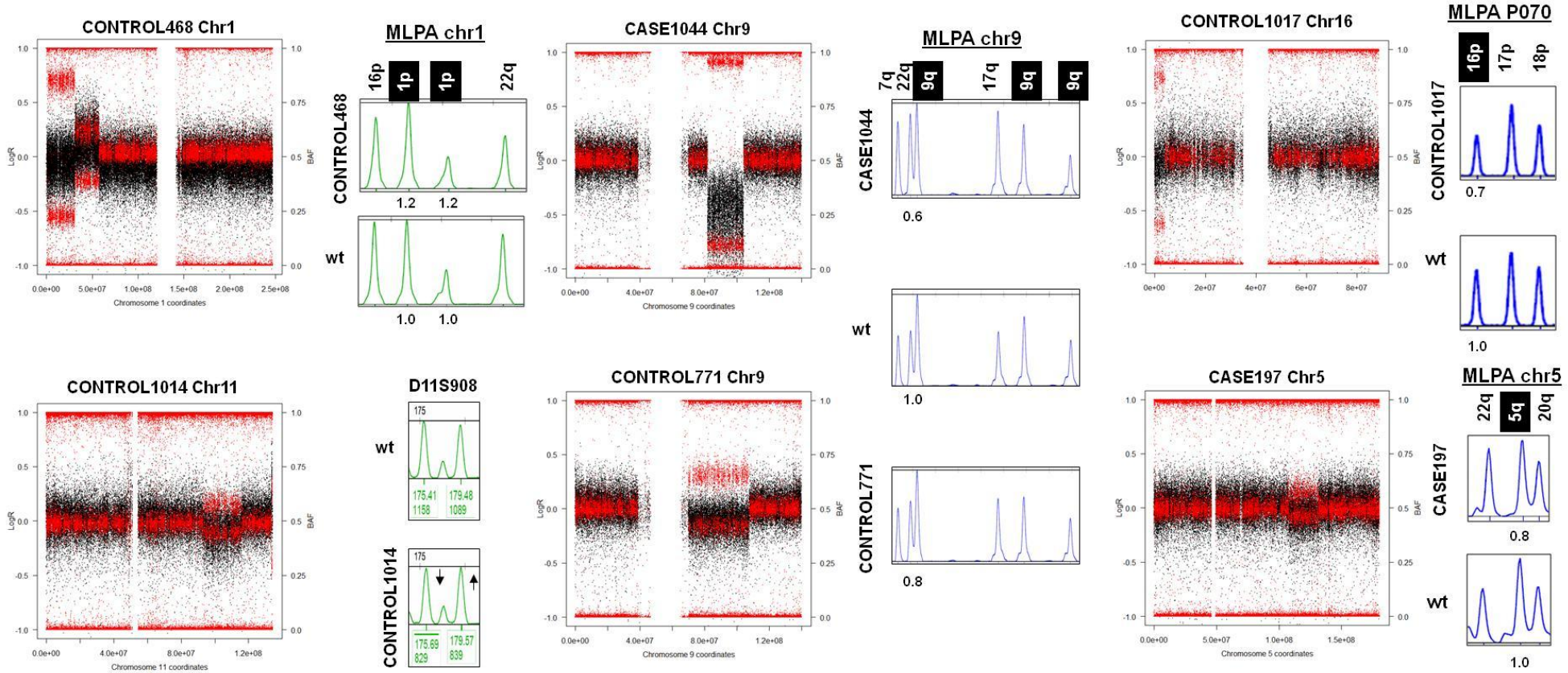


Figure S3D. Mosaic UPDs

Mosaic UPDs at 17q in CONTROL1007 and CONTROL369, 17p in CASE962 and CASE815, 19q in CONTROL670, and 21q in CASE138. MLPA confirmed the disomic state at the UPD loci with no gain or loss of genetic material (~1.0 RPH), while microsatellite analysis ratified the allelic imbalance reflected by an aberrant ratio between allelic peaks with respect to the wild-type pattern in CONTROL1007 and in two different tissues (blood and bladder) of two individuals shown (CASE962 and CASE815).



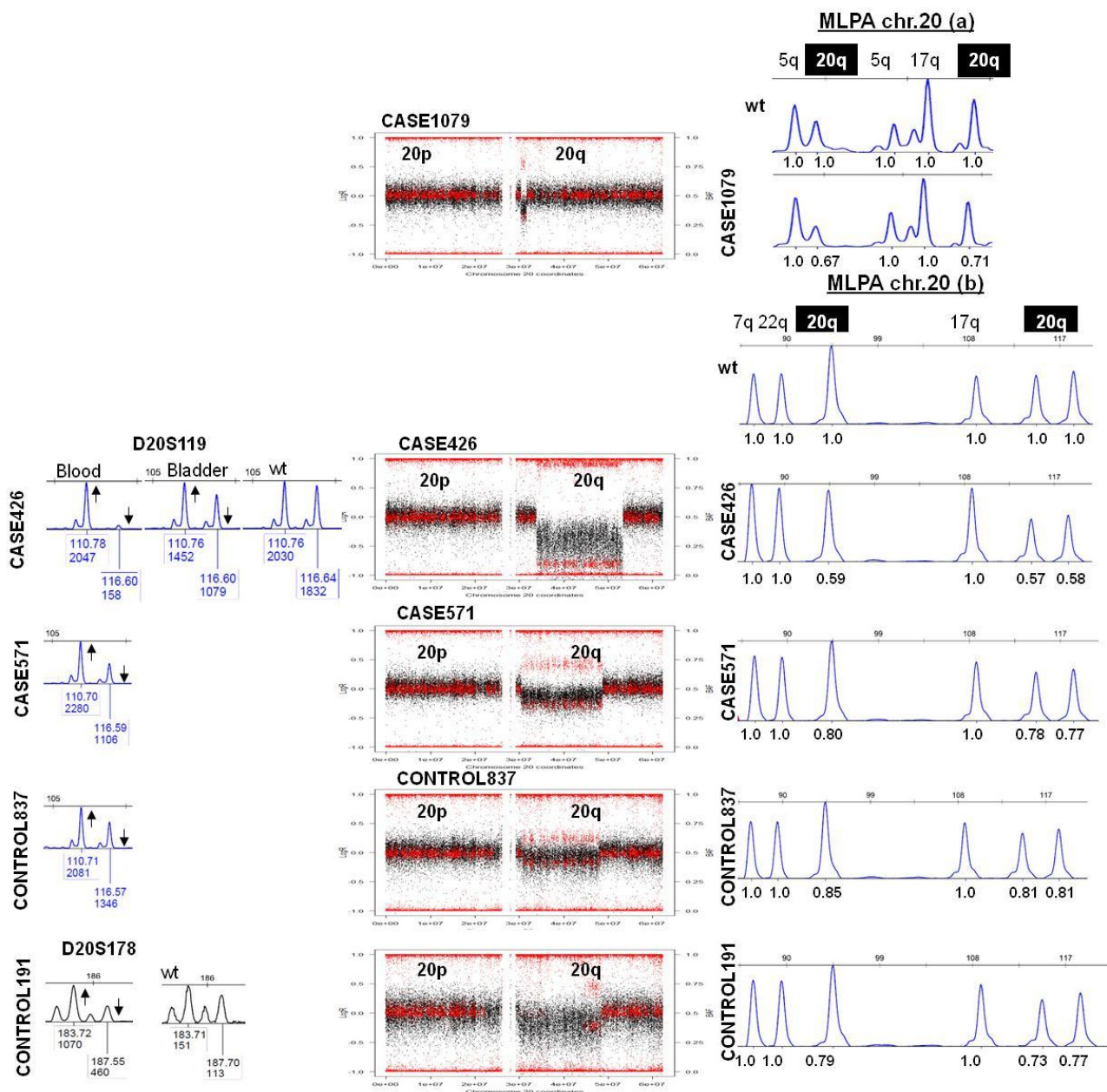


Figure S3F. Mosaic chr20 CNVs

A loss of genetic material from chromosome 20q is revealed by MLPA (RPHs between 0.57 and 0.85) in all 5 detected samples. Microsatellite analysis in blood (4 individuals) and bladder (CASE426) ratified an allelic imbalance with respect to the wild-type pattern.

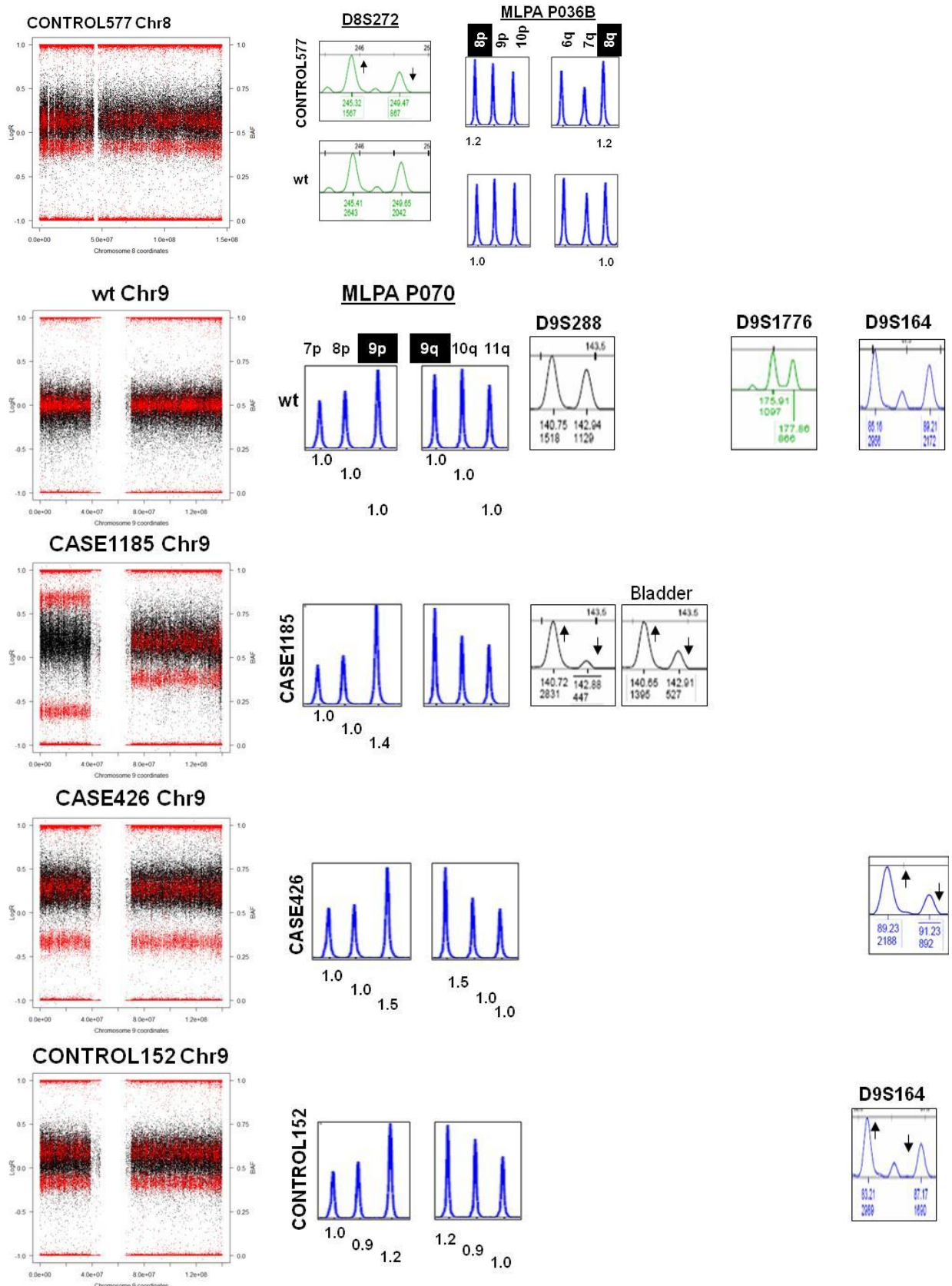


Figure S3G. Mosaic Trisomies

Mosaic trisomies (polysomies?). MLPA confirmed a gain of genetic material at the trisomic loci ($RPH > 1.2$) while microsatellite analysis ratified the allelic imbalance without detecting third alleles.

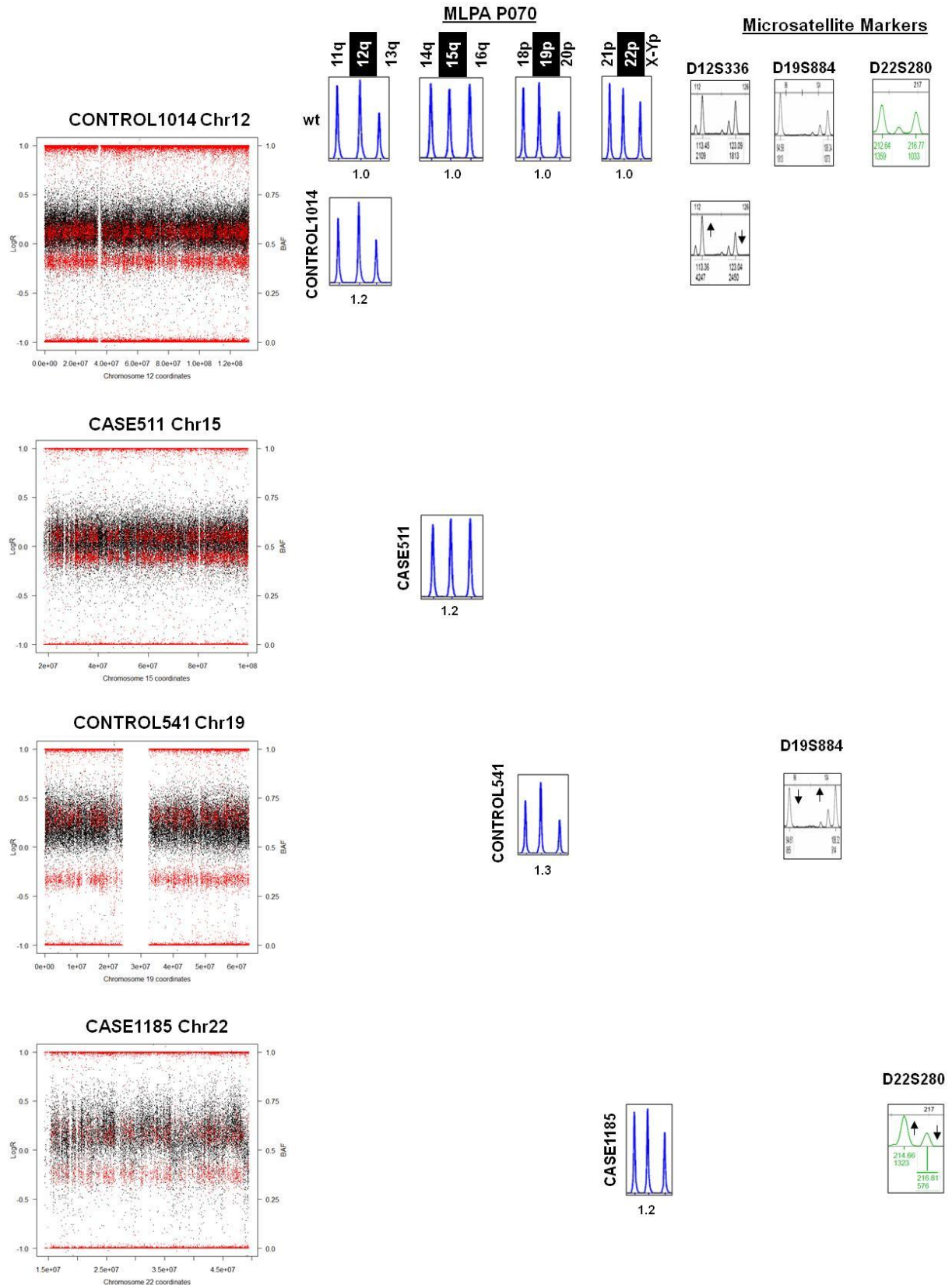


Table S1.

Chr	LogR	Bdev	HetBdev
1	-0.0185 ± 0.0369	0.0125 ± 0.0099	0.0344 ± 0.0124
2	-0.021 ± 0.0389	0.0125 ± 0.0099	0.0333 ± 0.0123
3	-0.0208 ± 0.0398	0.0125 ± 0.0099	0.0331 ± 0.0123
4	-0.025 ± 0.0446	0.0127 ± 0.0099	0.0336 ± 0.0123
5	-0.0219 ± 0.0402	0.0125 ± 0.0099	0.0332 ± 0.0123
6	-0.0228 ± 0.039	0.0131 ± 0.0099	0.035 ± 0.0122
7	-0.0214 ± 0.0391	0.0133 ± 0.0099	0.0355 ± 0.0126
8	-0.0207 ± 0.0394	0.0124 ± 0.0099	0.0328 ± 0.0123
9	-0.02 ± 0.0387	0.0127 ± 0.01	0.0336 ± 0.0131
10	-0.0185 ± 0.0372	0.0125 ± 0.0099	0.0335 ± 0.0122
11	-0.0209 ± 0.0372	0.0128 ± 0.0099	0.0344 ± 0.0123
12	-0.0195 ± 0.0376	0.0125 ± 0.0099	0.0339 ± 0.0124
13	-0.0228 ± 0.0425	0.0124 ± 0.01	0.0325 ± 0.0125
14	-0.0212 ± 0.038	0.0125 ± 0.0099	0.0334 ± 0.0126
15	-0.0181 ± 0.037	0.0127 ± 0.0098	0.0345 ± 0.0123
16	-0.0192 ± 0.0398	0.0132 ± 0.0099	0.0363 ± 0.0124
17	-0.0179 ± 0.0404	0.0134 ± 0.0099	0.037 ± 0.0125
18	-0.0204 ± 0.0397	0.0122 ± 0.0099	0.0321 ± 0.0123
19	-0.0215 ± 0.051	0.0152 ± 0.0102	0.0427 ± 0.0139
20	-0.0181 ± 0.0387	0.0123 ± 0.01	0.0331 ± 0.0125
21	-0.0216 ± 0.0394	0.0133 ± 0.0099	0.0342 ± 0.0122
22	-0.0197 ± 0.0475	0.0136 ± 0.01	0.0368 ± 0.0127

Mean and standard deviation (SD) of log R ratio (LogR), B-deviation (Bdev) and B-deviation of heterozygous SNPs (HetBdev) per autosomal chromosome of the 1,991 samples analysed. Data are presented as mean ± SD.

Table S2. Mosaic rearrangements detected in cases and controls, divided by categories with information about the validation methods used (microsatellites, MLPA and/or FISH), chromosomal coordinates and size of the rearrangement, and actual LogR and Heterozygous B-deviation values obtained with the SNP array.

Microarray Values shown per sample (columns 10-17): **LogR sample:** Mean LogR from all autosomal probes of the array (chr1-22) in the sample; **LogR mosaic:** Mean LogR from all probes within the rearranged region; **LogR chr dataset:** Mean LogR from all probes of the chromosome analysed in the whole dataset; **LogR SD chr dataset:** Standard Deviation (SD) from mean LogR of whole dataset; **HetBdev sample:** Mean B-deviation from autosomal heterozygote probes (chr1-22) of the mosaic sample; **HetBdev mosaic:** Mean B-deviation from heterozygote probes within the mosaic region; **HetBdev chr dataset:** Mean B-deviation of heterozygote probes from the chromosome analysed in whole dataset; **HetBdev SD chr dataset:** SD from mean B-deviation of heterozygote probes from the chromosome analysed in whole dataset.

Concordance/Confirmation of the rearrangements by independent experimental methods (**columns 3-5**): Microsatellite markers (**Micros.**), Multiplex Ligation Probe-dependent Amplification (**MLPA**) and/or fluorescence In Situ Hybridisation (**FISH**). FISH experiments were performed in bladder tissue. MLPA probemixes used included the commercial subtelomeric panels P70 and P36B (MRC-Holland) and custom made chr7 (19 probes); chr17 (1 probe), chr20 (3 probes) and chr22 (11 probes) panels.

Table S2A. Mosaic uniparental disomies detected showing normal LogR (copy number neutral) and abnormal heterozygous B-deviation parameters when compared to the genome-wide hybridization data of the sample and to the whole dataset.

sampleID	rearrangement	Micros.	MLPA	FISH	Chr	start	end	Size (Mb)	LogR_sample	LogR_mosaic	LogR_chr_dataset	LogR_SD_chr_dataset	HetBdev_sample	HetBdev_mosaic	HetBdev_chr_dataset	HetBdev_SD_chr_dataset
CONTROL468	UPD	YES	YES		1	1	31,505,375	31.5	-0.067	-0.063	-0.019	0.037	0.044	0.3	0.034	0.012
CONTROL776	UPD	NA	YES		2	1	5,974,108	5.9	0.003	-0.014	-0.021	0.039	0.041	0.127	0.033	0.012
CONTROL196	UPD	YES	YES		2	210,669,755	242,951,149	32.2	-0.001	0.013	-0.021	0.039	0.042	0.259	0.033	0.012
CASE954	UPD	NI	YES		2	218,476,667	242,951,149	24.4	-0.004	0.001	-0.021	0.039	0.034	0.106	0.033	0.012
CASE155	UPD	NA	YES		3	1	43,770,009	43.3	-0.017	-0.011	-0.021	0.04	0.032	0.063	0.033	0.012
CASE1105	UPD	NA	YES		7	62,401,114	96,812,073	34.4	-0.049	-0.019	-0.021	0.039	0.03	0.148	0.036	0.013
						96,934,617	158,821,424	61.8	-0.049	-0.047	-0.021	0.039	0.03	0.086	0.036	0.013
CONTROL468	UPD	NA	YES		7	69,769,236	158,821,424	89	-0.067	-0.06	-0.021	0.039	0.044	0.303	0.036	0.013
CONTROL586	UPD	NA	YES		9	1	39,102,964	39.1	-0.025	-0.019	-0.02	0.039	0.03	0.347	0.034	0.013
CONTROL843	UPD	NA	YES		11	65,547,103	134,452,384	68.9	-0.045	-0.037	-0.021	0.037	0.036	0.099	0.034	0.012
CASE125	UPD	NA	YES		12	55,481,646	132,349,534	76.8	-0.046	-0.045	-0.02	0.038	0.027	0.06	0.034	0.012
CASE234	UPD	NA	YES		13	17,956,717	114,142,980	96.1	0.012	0.019	-0.023	0.043	0.029	0.053	0.033	0.013
CASE962	UPD	YES	NA		13	19,554,439	114,142,980	94.5	0.021	0.034	-0.023	0.043	0.035	0.136	0.033	0.013
CASE787	UPD	NI	YES		14	23,303,146	106,368,585	83	-0.052	-0.051	-0.021	0.038	0.032	0.164	0.033	0.013
CASE758	UPD	YES	YES		14	74,454,224	106,368,585	31.9	-0.005	-0.016	-0.021	0.038	0.01	0.081	0.033	0.013
CASE1205	UPD	YES	YES		16	1	14,565,117	14.5	-0.032	-0.076	-0.019	0.04	0.037	0.065	0.036	0.012
CASE962	UPD	YES	NA		17	1	18,649,825	18.6	-0.079	-0.036	-0.018	0.04	0.03	0.202	0.037	0.013
CASE815	UPD	YES	YES	YES	17	1	4,724,664	4.7	0.021	-0.003	-0.018	0.04	0.035	0.134	0.037	0.013
CASE369	UPD	NI	YES		17	37,339,650	78,774,742	41.4	0.017	0.019	-0.018	0.04	0.027	0.116	0.037	0.013
CONTROL1007	UPD	YES	YES		17	53,007,738	78,774,742	25.7	-0.066	-0.074	-0.018	0.04	0.032	0.098	0.037	0.013
CONTROL670	UPD	NA	YES		19	48,312,997	63,811,651	15.4	0.017	0.018	-0.022	0.051	0.026	0.09	0.043	0.014
CASE138	UPD	NA	YES		21	31,600,986	46,944,323	15.3	0.006	0.028	-0.022	0.039	0.029	0.09	0.034	0.012

Table S2B. Mosaic copy number change rearrangements affecting autosomes, showing slightly abnormal LogR values under the CNV call cut-off along with abnormal heterozygous B-deviation parameters when compared to the genome-wide hybridization data of the sample and to the whole dataset.

^aRegion of complete homozygosity, compatible with non-mosaic UPD or identity by descent (IBD), overlapping with the interstitial mosaic deletion below.

UPD: Uniparental Disomy, NA: Not Analysed; NI: Not Informative (homozygous marker).

sampleID	rearrangement	Micros.	MLPA	FISH ^b	chr	start	end	Size (Mb)	LogR_sample	LogR_mosaic	LogR_chr_dataset	LogR_SD_chr_dataset	HetBdev_sample	HetBdev_mosaic	HetBdev_chr_dataset	HetBdev_SD_chr_dataset
CONTROL468	duplication	NA	YES		1	31,508,099	58,012,249	26.3	-0.067	0.105	-0.019	0.037	0.044	0.119	0.034	0.012
CASE197	deletion	NA	YES		5	107,759,583	131,76,9397	24	-0.009	-0.076	-0.022	0.040	0.032	0.089	0.033	0.012
CONTROL771	deletion	NA	YES		9	70,096,379	107,838,079	37.7	0.009	-0.135	-0.020	0.039	0.029	0.119	0.034	0.013
CASE1044	deletion	NA	YES		9	82,074,397	104,355,425	22.2	-0.008	-0.489	-0.020	0.039	0.029	0.352	0.034	0.013
CONTROL1014	deletion	YES	NA		11	93,126,656	116,093,059	22.9	0.004	-0.097	-0.021	0.037	0.04	0.072	0.034	0.012
CONTROL1017	deletion	NA	YES		16	1	3,888,919	3.8	0.007	-0.087	-0.019	0.040	0.035	0.315	0.036	0.012
CASE1079	deletion	NA	YES		20	30,488,149	31,745,200	1.2	-0.004	-0.26	-0.018	0.039	0.03	0.227	0.033	0.012
CASE571	deletion	YES	YES		20	30,491,175	48,812,965	18.3	0.01	-0.163	-0.018	0.039	0.034	0.173	0.033	0.012
CONTROL837	deletion	YES	YES		20	30,824,044	48,140,963	17.3	0.005	-0.120	-0.018	0.039	0.04	0.116	0.033	0.012
CASE426	deletion	YES	YES	YES	20	33,993,320	53,443,077	19.4	-0.01	-0.483	-0.018	0.039	0.04	0.351	0.033	0.012
CONTROL191	UPD/IBD ^a	YES	YES		20	22,351,287	44,783,987	22.4	-0.017	-0.015	-0.018	0.039	0.047	-	0.033	0.012
	deletion	YES	YES		20	30,488,149	48,812,965	18.3	-0.017	-0.205	-0.018	0.039	0.047	0.167	0.033	0.012
CONTROL577	trisomy	YES	YES		8	1	146,274,826	146.3	0.013	0.127	-0.021	0.039	0.037	0.083	0.033	0.012
CASE1185	trisomy	YES	YES	YES	9	1	140,273,252	140.3	-0.013	0.159	-0.020	0.039	0.041	0.189	0.034	0.013
CASE426	trisomy	YES	YES	YES	9	1	140,273,252	140.3	-0.01	0.269	-0.020	0.039	0.04	0.154	0.034	0.013
CONTROL152	trisomy	NI	YES		9	1	140,273,252	140.3	-0.04	0.105	-0.020	0.039	0.038	0.094	0.034	0.013
CONTROL1014	trisomy	YES	YES		12	1	132,349,534	132.3	0.004	0.129	-0.020	0.038	0.04	0.084	0.034	0.012
CASE511	trisomy	NA	YES		15	1	100,338,915	100.3	-0.042	0.053	-0.018	0.037	0.03	0.064	0.035	0.012
CONTROL541	trisomy	YES	YES		19	1	63,811,651	63.8	-0.026	0.222	-0.022	0.051	0.035	0.162	0.043	0.014
CASE1185	trisomy	YES	YES		22	1	49,691,432	49.7	-0.013	0.136	-0.020	0.047	0.041	0.109	0.037	0.013

Table S3. Statistical tests for case-control comparisons of mosaic rearrangement frequency and proportion of cells carrying the rearrangement

Fisher's test for count data

	Deletion	no CNV	Trisomy+Dup	no TRIS	UPD	no UPD	Any event	no event
CASES	5	1029	3	1031	12	1022	19	1015
CONTROLS	5	952	5	952	7	950	15	942
OR	0.925 (0.212-4.033)		0.554 (0.085-2.857)		1.593 (0.624-4.064)		1.175(0.593-2.326)	
p-values		1.000		0.492		0.450		0.764

Welch two sample t-test for differences in the proportion of cells carrying each type of mosaic rearrangement

	t	df	p
Deletions	1.561	5.448	0.174
Trisomies+Duplicates	0.219	6.470	0.833
UPDs	-2.028	7.892	0.077

Table S4. Genomic location and sequence characteristics of the breakpoint (BP) intervals for each somatic rearrangement

Rearrangement	Chr	BP location range	Genomic feature	Gene or genomic sequence
duplication	1p	31505375-31508099 58012249-58020360	CNV MRH	Within the <i>SNRNP40</i> gene Within the <i>DAB1</i> gene
deletion	5q	107751916-107759583 131769397-131780519	- -	Gene desert region (>100kb) Within the <i>C5orf56</i> gene
deletion	9q	70093133-70096379 107838079-107840864	SD, CNV	Within the <i>CBWB3</i> gene, SD close to the centromere Gene desert region (>500kb)
deletion	9q	82074032-82074397 104355425-104357470	- -	Gene desert region (>1500kb) Gene desert region (>1000kb)
deletion	11q	93121041-93126656 116093059-116094337	- -	Within the <i>C11orf54</i> gene Gene desert region (>1000kb)
deletion	16p	3888919-3902621	MRH ^d	Intergenic, between <i>CREBBP</i> & <i>ADCY9</i> genes
deletion	20q	30486620-30488149 31745200-31748231	- -	Within the <i>ASXL1</i> gene Intergenic, between <i>E2F1</i> & <i>PXMP4</i> genes
deletion ^a	20q	30489196-30491175 48812965-48815555	- MRH ^d , SD ^d , (CNV)	Within the <i>ASXL1</i> gene Intergenic, between <i>PARD6B</i> & <i>BCAS4</i> genes
deletion	20q	30823358-30824044 48140963-48144977	(CNV) (CNV)	Within the <i>DNMT3B</i> gene Within the <i>UBE2V1</i> gene
deletion	20q	33985474-33993320 53443077-53451892	(CNV) -	Within the <i>PHF20</i> gene Gene desert region (>1000kb)
UPD	1p	31505375-31508099	CNV	Within the <i>SNRNP40</i> gene
UPD	2p	5974108-5987460	MRH ^d	Intergenic, between the <i>SOX11</i> and <i>LOC150622</i> genes
UPD	2q	210669755-210673136	-	Within the <i>C2orf67</i> gene
UPD	2q	218461881-218476667	-	Within the <i>TNS1</i> gene
UPD	3p	43770009-43771496	MRH	Intergenic, between the <i>ABHD5</i> and <i>C3orf77</i> genes
UPD	7q	62326882-62401114 7q 96812073-96821617	SD, CNV MRH	In a large SD cluster close to cen Gene desert region (>500kb)
UPD	7q	69763300-69769236	MRH ^d	Within the <i>AUTS2</i> gene
UPD ^b	9p	39102964-39139209	SD, CNV	Region rich in SD up to the centromere
UPD	11q	65433092-65547103 ^c	MRH ^d , CNV ^d	Interval containing 7 genes, <i>C11orf68</i> to <i>CATSPER1</i>
UPD	12q	55476810-55481646	-	Intergenic, between <i>HSD17B6</i> & <i>SDR9C7</i> genes
UPD	13q	17922259-17956717	SD, CNV	Region rich in SD up to the centromere
UPD	13q	19515797-19554439	-	Within the <i>ZMYM2</i> gene
UPD	14q	23294523-23303146	MRH ^d	Intergenic, between <i>DHRS2</i> & <i>C14orf165</i> genes
UPD	14q	74448100-74454224	-	Within the <i>RPS6KL1</i> gene
UPD	16p	14565117-14572980	(CNV)	Within the <i>PARN1</i> gene
UPD	17p	18649825-18659852	SD, CNV	Within the <i>LLG1</i> gene
UPD	17p	4724664-4736083	CNV	Within the <i>MINK1</i> gene
UPD	17q	37211915-37339650 ^c	-	Interval containing 6 genes, <i>SC65</i> to <i>ACLY</i>
UPD	17q	52969779-53007738	(CNV)	Within the <i>MSI2</i> gene
UPD	19q	48275526-48312997	SD, CNV	Cluster of PSG gene copies in SD
UPD	21q	31595718-31600986	SD	Within the <i>TIAM1</i> gene

Meiotic recombination hotspots (MRH), averaged across populations, were obtained from the HapMap website. The width of a hotspot represents the region where the estimated rate is within a factor of two of the maximum (Myers *et al*, Science 2010). We defined a rearrangement breakpoint interval as coincidental with a specific genomic feature or sequence (SD, MRH, CNV, gene) when more than 50% of the feature overlapped with the breakpoint interval between.

MRH: meiotic recombination hotspot. **SD:** segmental duplication. **CNV:** copy number variation

^aAlmost identical 20q deletion detected in two samples (case571 and control191)

^bAlmost identical 9p UPD detected in two samples

^cA relatively poor definition of the breakpoint interval (>100kb) in two UPD samples was due to the presence of stretches of homozygosity (uninformative SNPs) in the region.

^dThe feature encompasses less than 50% of the defined breakpoint interval. CNVs only reported with BAC arrays, whose boundaries are probably not well defined, are shown between brackets.

Table S5. Coordinates of MLPA and microsatellite PCR products (hg18 assembly)

Name	Chr	start_product	end_product
FISH			
CTD-2009B12	17	371,341	489,193
CTD-2556K12	17	551,111	747,647
RP11-216P6	17	814,501	916,339
RP11-85C21	9	126,320,900	126,493,771
RP11-634C23	9	126,511,066	126,654,826
RP11-346B17	9	126,774,264	126,941,040
RP11-116O13	20	43,536,601	43,730,870
RP11-103O9	20	43,833,556	44,008,890
RP11-702N24	22	17,298,032	17,448,439
RP11-800B2	22	17,466,004	17,647,712
RP11-479G10	22	17,630,839	17,818,820
MLPA			
HDAC1 exon6	1	32,565,785	32,565,866
CDCA8	1	37,943,701	37,943,757
PRR16	5	119,828,162	119,828,215
SEMA6A	5	115,846,143	115,846,142
AUTS2	7	69,884,540	69,884,599
WBSCR17	7	70,235,725	70,235,777
FKBP6	7	72,392,746	72,392,793
BAZ1B	7	72,563,035	72,563,100
WBSCR14	7	72,668,338	72,668,383
WBSCR22	7	72,745,566	72,745,619
STX1A	7	72,761,324	72,761,380
LIMK1	7	73,136,250	73,136,311
WBSCR1	7	73,242,518	73,242,565
RCF2	7	73,295,450	73,295,488
CYLN2	7	73,412,489	73,412,533
GTF2IRD1	7	73,560,406	73,560,449
GTF2I	7	73,769,150	73,769,203
WBSCR16	7	74,124,453	74,124,512
HIP1	7	75,059,659	75,059,715
TRIM56	7	100,519,362	100,519,417
EMID2	7	100,849,979	100,850,030
CUTL1	7	101,679,399	101,679,455
PRK RIP1	7	101,827,026	101,827,097
SCNN1G	16	23,108,201	23,108,259
MAPT	17	41,458,365	41,458,434
SPAG4L	20	31,037,243	31,037,299
SNTA1	20	31,489,063	31,489,119
PPGB	20	43,954,792	43,954,845
PLTPb	20	43,961,027	43,961,085
PLTP	20	43,968,347	43,968,404
HIRA	22	17,693,525	17,693,575
RP11-652F11	22	18,029,000	18,029,066
COMT	22	18,330,070	18,330,129
ZDHHC8	22	18,508,156	18,508,215
RP11-307O16	22	20,832,866	20,832,924
RP11-757F24	22	21,151,921	21,151,975
RP11-281O23	22	21,286,912	21,286,964
RP11-50L23	22	21,434,354	21,434,413
RP11-264C20	22	21,521,303	21,521,350

RP11-165G05	22	21,650,048	21,650,112
GNB1L	22	18,169,603	18,169,662
SHANK3	22	49,461,919	49,461,975

MRC-Holland MLPA

P036B: All subtelomeric regions and pseudoautosomal regions

P070: All subtelomeric regions and pseudoautosomal regions

Microsatellite Markers

D1S2667	1	11,409,625	11,409,894
D1S199	1	19,829,636	19,829,735
D2S396	2	230,391,872	230,392,111
D2S338	2	236,900,151	236,900,439
D5S471	5	118,976,843	119,177,177
D8S264	8	2,117,740	2,117,874
D8S505	8	34,570,543	34,570,687
D8S514	8	123,811,415	123,811,633
D8S272	8	137,804,548	137,804,711
D9S288	9	3,941,792	3,941,919
D9S286	9	8,043,436	8,043,574
D9S1776	9	116,999,255	116,999,373
D9S164	9	135,245,780	135,245,933
D11S898	11	100,561,808	100,561,956
D11S908	11	114,792,573	114,792,698
D12S336	12	9,385,421	9,385,618
D12S364	12	13,724,592	13,724,744
D12S79	12	114,544,838	114,545,000
D12S86	12	117,654,705	117,654,838
D13S263	13	40,978,976	40,979,126
D13S170	13	80,007,129	80,007,346
D13S158	13	102,774,399	102,774,509
D13S285	13	111,843,433	111,843,541
D14S283	14	21,757,385	21,757,515
D14S258	14	69,652,764	69,652,939
D14S68	14	87,697,518	87,697,683
D14S292	14	103,566,457	103,766,715
D14S985	14	100,266,289	100,466,568
D16S423	16	5,883,142	6,083,470
D17S849	17	346,160	346,416
D17S831	17	1,806,767	1,806,994
D17S1828	17	3,700,488	3,700,696
D17S921	17	14,201,467	14,201,613
D17S787	17	50,637,083	50,637,234
D17S785	17	71,942,972	71,943,161
D17S784	17	75,316,716	75,517,019
D19S884	19	8,056,011	8,056,236
D19S221	19	12,573,793	12,573,991
D19S902	19	53,023,869	53,024,083
D19S571	19	57,988,784	57,989,011
D20S107	20	38,315,955	38,316,159
D20S119	20	43,082,466	43,082,583
D20S178	20	45,985,389	45,985,642
D20S196	20	48,995,183	48,995,325
D22S420	22	16,239,503	16,239,639
D22S315	22	24,345,881	24,346,065
D22S280	22	31,539,423	31,539,626
D22S283	22	35,080,895	35,081,028